Properties of *S* waves near a kiss singularity: comparison of exact and ray solutions

Václav Vavryčuk

Geophysical Institute, Academy of Sciences of the Czech Republic, Boční II/1401, 141 31 Praha 4, Czech Republic; e-mail: vv@ig.cas.cz

SUMMARY

We study properties of *S* waves generated by a point source in a homogeneous transversely isotropic medium and propagating in directions close to a kiss singularity which coincides with the symmetry axis of the medium. Comparing an exact and ray solutions in the far field we show that the zeroth-order ray approximation fails for these directions. The wavefield of the *S* waves is not composed only of two split *S* waves, as is usually assumed, but contains also their interaction. The interaction wave appears in times between arrivals of the split *S* waves, it can be of high frequency and it can be detected in the near field but also in the far field. The split *S* waves are described by the zeroth-order ray approximation, the interaction wave can be successfully reproduced by the first-order ray approximation. In analogy to the near-field wave, which appears in the vicinity of a source, we call the interaction wave as the “near-singularity wave”, because it is prominent only in the vicinity of the *S*-wave singularity. The near-singularity wave is a non-geometrical wave, being described by higher-order ray approximations and neglected by the geometrical ray theory.

Key words: anisotropy, Green tensor, near-field wave, near-singularity wave, ray theory, *S*-wave splitting, *S*-wave singularity, *S*-wave coupling.

1 INTRODUCTION

The *S*-wave singularities are very important for modelling of *S* waves in anisotropic media. They are defined as the directions where *S* waves have coincident phase velocities, and they are very common in all types of anisotropy. For directions near the singularities, polarization of plane *S* waves can change very rapidly, and amplitude and polarization of *S* waves with curved wavefronts can behave quite anomalously (Crampin & Yedlin 1981). We distinguish kiss, point and line singularities (Crampin 1991), among them the point singularity affects geometry of rays and the wavefield in the most complicated and drastic way. It is known that standard ray theory is inapplicable for modelling the wavefield near the point singularity, thus other techniques like using the Radon transform (Wang & Achenbach 1994), reflectivity (Crampin 1991) or Maslov method (Rümpker & Thomson 1994) must be used. It is not clear, however, how much is the wavefield affected by the *kiss singularity*, which is defined as a direction where two *S*-wave phase-velocity sheets touch *tangentially* at isolated point. Since the group velocities near the kiss singularity behave quite regularly, it is believed that "the waveforms of initial shear-wave pulse will propagate with little distortion" and "the shear waves will split in a regular manner without any particular anomaly" (Crampin 1991). It would imply that the ray theory can be applied for modelling the wavefield near the kiss singularity.

In this paper we shall focus on the problem of applicability of the ray theory for modelling of *S* waves close to a kiss singularity. We shall study *S* waves generated by a point source situated in a homogeneous transversely isotropic medium (hereafter TI medium), where the kiss singularity coincides with the symmetry axis of the medium. Since the symmetry axis will be vertical, the split *S* waves become *SV* and *SH* waves with polarization vectors near the singularity as shown in Fig. 1. For this medium, we shall compare exact and ray solutions in the far field, and we shall show that the standard ray theory (meaning the zeroth-order ray approximation) fails in this case. However, if we include into the solution a new wave described by the first-order ray approximation and calculated by Vavryčuk & Yomogida (1996) and by Vavryčuk (1997), then we obtain a correct result. This non-geometrical wave is called the "near-singularity" wave, it has a simple analytical form and its properties are in detail discussed.

2 THEORY

2.1 Exact integral solution of the Green tensor

The exact elastodynamic Green tensor $G_{ij}(\mathbf{x},t)$ for homogeneous anisotropic media can be expressed as follows (Burridge 1967, Eq. 4.6; Wang & Achenbach 1994, Eq. 13)

$$G_{kl}(\mathbf{x},t) = -\frac{H(t)}{8\pi^2\rho}\int\limits_{|\mathbf{n}|=1}\sum_{m=1}^{3}\frac{g_k^m g_l^m}{\left(c^m\right)^3}\,\dot{\delta}\left(t-\frac{\mathbf{n}\cdot\mathbf{x}}{c^m}\right)d\mathbf{n}\ , \tag{1}$$

where m = 1,2,3 denotes the type of the wave (*P*, *S*1 and *S*2), **g** denotes the unit polarization vector, *c* is the phase velocity, ρ is the density of the medium, *t* is time, $H(t)$ is the Heaviside step function, $\dot{\delta}(t)$ is the time derivative of the Dirac delta function, **x** is the position vector of an observation point, and **n** is the phase normal. The integral area is a unit sphere. Eq. (1) represents an exact and complete solution for homogeneous weakly as well as strongly anisotropic medium, containing far-field as well as near-field waves and being valid at all distances and directions including the shear-wave singularity direction. For an *isotropic medium*, the integral (1) can be solved analytically, and the well-known Stokes solution is then obtained (see Mura 1991, pp. 61-63; Červený 1997, Sec. 2.5.4). For a *transversely isotropic medium* with a vertical axis of symmetry, the integral (1) has also been solved analytically but only for the symmetry axis direction (Payton 1977). For the other directions the integral should be solved either numerically or it should be expanded asymptotically.

2.2 Far-field approximation versus zeroth-order ray approximation

Solving the exact integral form of the Green tensor (1) by the stationary phase method we obtain the *far-field approximation of the Green tensor* in the following form (Kendall, Guest & Thomson 1992, Eq. 1):

$$G_{kl}^{far}(\mathbf{x},t) = \frac{1}{4\pi\rho}\sum_{m=1}^{3}\frac{1}{v^m\sqrt{K_p^m}}\frac{g_k^m g_l^m}{r}\delta\left(t-\tau^m(\mathbf{x})\right)\ , \tag{2}$$

where v is the group velocity, $\mathbf{g}$ is the unit polarization vector, K_p is the Gaussian curvature of the slowness surface, r is the distance of an observation point from the source, $\delta(t)$ is the Dirac delta function, and τ is the traveltime. Superscript *m* denotes again the type of the wave. Eq. (2) is valid for all directions, except of the vicinity of singular points where another formula must be used (Červený 1997, p. 88).

Now we are faced at the question, how to define the *zeroth-order ray-theoretical Green tensor* $G_{kl}^{(0)}(\mathbf{x},t)$, from which the whole ray series is then constructed (see Vavryčuk & Yomogida 1996). The most common way is to define the zeroth-order term of the ray series by Eq. (2) for directions far from the singular points, and by another formula for directions close to the singularity. Thus the wavefield will be described by two different ray solutions with different and limited regions of applicability. Moreover, for directions in between (not close but also not far from the singular direction) we obtain a gap with no satisfactory ray solution. It is highly desirable, however, to have only one ray solution describing the wavefield in all directions including singular points. Therefore, we use another approach in this paper. We define the zeroth-order ray-theoretical Green tensor $G_{kl}^{(0)}(\mathbf{x},t)$ by formula (2) not only for regular directions but also for directions close to the singularity or even in the singular direction. As a consequence, the *zeroth-order ray approximation will differ from the far-field approximation for directions close to the singularity.* This inconsistency will be, however, corrected by including higher-order ray approximations. We shall show that *it is really possible to write only one ray solution which describes the far-field waves correctly for all directions including the singularity.*

2.3 The zeroth-order ray theoretical Green tensor in TI medium

In the case of a homogeneous transversely isotropic medium with a vertical axis of symmetry, the *S*1 and *S*2 waves become the *SV* and *SH* waves and all quantities in Eq. (2) can be expressed analytically. For the *SH* waves, we obtain (Vavryčuk & Yomogida 1996, Eq. 25):

$$G_{kl}^{SH(0)}(\mathbf{x},t) = \frac{1}{4\pi\rho}\,\frac{1}{a_{66}\sqrt{a_{44}}}\,\frac{g_k^{SH} g_l^{SH}}{\tau^{SH}}\;\delta\left(t-\tau^{SH}\right), \tag{3}$$

where $\mathbf{g}^{SH} = \left(\sin\varphi, -\cos\varphi, 0\right)^T$ and $\tau^{SH} = r\sqrt{\dfrac{\sin^2\vartheta}{a_{66}} + \dfrac{\cos^2\vartheta}{a_{44}}}$.

Quantities a_{kl} denote the two-index notation of the density-normalized elastic parameters (see Červený, Molotkov & Pšenčík 1977, pp. 165-166), ϑ and φ are the standard spherical angles of the position vector $\mathbf{x}$ of an observation point, and the point source is situated in the origin of coordinates.

For the *P* and *SV* waves, the formulae are rather cumbersome, because analytical formulae for group velocity v and Gaussian curvature K_p are rather long and complicated. The formulae are considerably simplified if we assume that the observation point lies in the symmetry axis direction, $\vartheta = 0$. For the complete *zeroth-order ray-theoretical Green tensor* in the singular direction we obtain:

$$G_{11}^{(0)}(z,t) = G_{11}^{SV(0)}(z,t),\; G_{22}^{(0)}(z,t) = G_{22}^{SH(0)}(z,t),\; G_{33}^{(0)}(z,t) = G_{33}^{P(0)}(z,t), \tag{4}$$

where

$$G_{11}^{SV(0)}(z,t) = \frac{1}{4\pi\rho}\left[a_{11} + \frac{(a_{13}+a_{44})^2}{a_{33}-a_{44}}\right]^{-1} \frac{\delta\left(t - \frac{|z|}{\sqrt{a_{44}}}\right)}{|z|}, \; G_{22}^{SH(0)}(z,t) = \frac{1}{4\pi\rho}\frac{1}{a_{66}}\frac{\delta\left(t - \frac{|z|}{\sqrt{a_{44}}}\right)}{|z|},$$

$$G_{33}^{P(0)}(z,t) = \frac{1}{4\pi\rho}\left[a_{44} + \frac{(a_{13}+a_{44})^2}{a_{33}-a_{44}}\right]^{-1} \frac{\delta\left(t - \frac{|z|}{\sqrt{a_{33}}}\right)}{|z|}, \tag{5}$$

other components of the Green tensor being zero. In Eqs (4) and (5) we used the following basis of polarization vectors: $\mathbf{g}^P = (0,0,1)^T, \mathbf{g}^{SV} = (1,0,0)^T$, $\mathbf{g}^{SH} = (0,-1,0)^T$.

Seemingly, we got an unphysical result for *S* waves in Eq. (5). For the propagation of waves along the symmetry axis, no direction in the *x-y* plane is preferential, thus components in the far field $G_{11}(z,t)$ and $G_{22}(z,t)$ must be equal, but we obtained $G_{11}^{(0)}(z,t) \neq G_{22}^{(0)}(z,t)$. The reason lies in the fact that in the vicinity of the *S*-wave singularity the zeroth-order ray approximation is not equivalent to the far-field approximation. In the next we show that for these exceptional directions not only the zeroth-order ray approximations but also higher-order ray approximations contribute to the far field.

2.4 The near-singularity wave

The *first-order ray approximation of the Green tensor* for homogeneous TI medium consists of two terms (Vavryčuk 1997): the first term describes a near-field wave, the second term describes an interaction between the *SV* and *SH* waves near the singular direction. Since we consider waves in the far field, we express only the interaction between the *SV* and *SH* waves (Vavryčuk & Yomogida 1996, Vavryčuk 1997):

$$G_{kl}^{S(1)}(\mathbf{x},t) = \frac{1}{4\pi\rho\sqrt{a_{44}}}\frac{g_k^{SH}g_l^{SH} - g_k^{SH\perp}g_l^{SH\perp}}{R^2}\left[H(t-\tau^{SH}) - H(t-\tau^{SV})\right], \tag{6}$$

where $\mathbf{g}^{SH\perp} = (\cos\varphi, \sin\varphi, 0)^T$ is the unit vector perpendicular to $\mathbf{g}^{SH} = (\sin\varphi, -\cos\varphi, 0)^T$, $R = r\sin\vartheta$ is the distance of an observation point from the singular direction, r is the distance of an observation point from the source, ϑ and φ are again the standard spherical angles of the $\mathbf{x}$ vector. It follows from Eq. (6) that the ray amplitude of this higher-order wave depends on the distance R of an observation point from the singular direction as $1/R^2$. Thus for observation points close to the singular direction this wave is most prominent. Moreover, even in the far field ($r \to \infty$) for which $R \to 0$, this wave can be non-negligible comparing to the zeroth-order waves. Therefore we shall call this non-geometrical wave as a "*near-singularity wave*".

Note that in Vavryčuk (1997) this wave is called the "*SV-SH coupling wave*", in analogy to the "*S-wave coupling*" introduced by Chapman & Shearer (1989) and Coates & Chapman (1990) for description of an interaction between the *S* waves in anisotropic *inhomogeneous* media. Not to mix the both effects together, we decided to use for the description of the *S*-wave interaction near the singularity in *homogeneous* anisotropic media consistently a term, the "near-singularity wave".

For the strictly singular direction Eq. (6) yields

$$G_{11}^{S(1)}(z,t)=\lim_{\vartheta\to 0} G_{11}^{S(1)}(\mathbf{x},t)=\frac{1}{4\pi\rho\sqrt{a_{44}}}\ \lim_{\vartheta\to 0}\left[\frac{\tau^{SH}-\tau^{SV}}{r^2\sin^2\vartheta}\right]\lim_{\vartheta\to 0}\left[\frac{H\left(t-\tau^{SV}\right)-H\left(t-\tau^{SH}\right)}{\tau^{SH}-\tau^{SV}}\right]=$$

$$=\frac{1}{8\pi\rho}\left\{\frac{1}{a_{66}}-\left[a_{11}-\frac{\left(a_{13}+a_{44}\right)^2}{a_{33}-a_{44}}\right]^{-1}\right\}\frac{\delta\left(t-\dfrac{|z|}{\sqrt{a_{44}}}\right)}{|z|}, \tag{7}$$

$$G_{22}^{S(1)}(z,t)=-G_{11}^{S(1)}(z,t)\ .$$

Interestingly, the *amplitude and the waveform of the near-singularity wave for the singular direction behave in the same way as a standard zeroth-order wave*. It is the reason, why this wave can be detected even in the far field. For the complete ray-theoretical Green tensor for the singular direction in the far field we then obtain

$$G_{11}^{far}(z,t)=G_{11}^{SV(0)}(z,t)+G_{11}^{S(1)}(z,t)=\frac{1}{8\pi\rho}\left\{\frac{1}{a_{66}}+\left[a_{11}-\frac{\left(a_{13}+a_{44}\right)^2}{a_{33}-a_{44}}\right]^{-1}\right\}\frac{\delta\left(t-\dfrac{|z|}{\sqrt{a_{44}}}\right)}{|z|},$$

$$G_{22}^{far}(z,t)=G_{22}^{SH(0)}(z,t)+G_{22}^{S(1)}(z,t)=\frac{1}{8\pi\rho}\left\{\frac{1}{a_{66}}+\left[a_{11}-\frac{\left(a_{13}+a_{44}\right)^2}{a_{33}-a_{44}}\right]^{-1}\right\}\frac{\delta\left(t-\dfrac{|z|}{\sqrt{a_{44}}}\right)}{|z|}, \tag{8}$$

$$G_{33}^{far}(z,t)=G_{33}^{P(0)}(z,t)=\frac{1}{4\pi\rho}\left[a_{44}+\frac{\left(a_{13}+a_{44}\right)^2}{a_{33}-a_{44}}\right]^{-1}\frac{\delta\left(t-\dfrac{|z|}{\sqrt{a_{33}}}\right)}{|z|}.$$

The correctness of the obtained far-field solution (8) for the singular direction was verified by comparing it with the exact Payton analytical solution (Payton 1977, 1983). *If we specify the Payton solution for the far field, then we obtain the identical result.*

2.5 The near-singularity wave versus the near-field wave

The near-singularity wave is similar in many aspects to the near-field wave. Therefore we shall summarize similarities and differences between the near-singularity and near-field waves (see Vavryčuk & Yomogida 1995,1996; Vavryčuk 1997):

1. Both kinds of waves are described by higher-order ray approximations, thus being neglected by the geometrical ray theory.
2. The amplitude of the near-field wave decreases with the distance from a point source as $1/r^2$, thus this wave is negligible far from the source.
3. The amplitude of the near-singularity wave decreases with the distance from a singular direction as $1/R^2$, thus this wave is negligible far from the singularity. Nevertheless, this wave can be significant in the near field as well as in the far field.
4. The near-singularity wave is a special wave, which can be classified neither as a pure near-field wave nor as a pure far-field wave. Properties of the near-singularity wave depend on the direction of propagation: for directions far from the singular direction the wave behaves like a

near-field wave, for directions close to the singular direction, the wave behaves like a far-field wave.

5. The frequency content of the near-singularity and near-field waves depends on separation times between the *P*- and *S*-wave arrivals, or between the *S*1- and *S*2-wave arrivals, respectively. For a small separation, the waves are rather of high frequency, for a large separation the waves are rather of low frequency. For the singular direction, the near-singularity wave contains the same frequencies as the zeroth-order waves.
6. Amplitude of the near-singularity wave depends on the strength of anisotropy: for strong anisotropy the wave is more pronounced. For a limit from anisotropy to isotropy the wave vanishes.

3 NUMERICAL MODELLING

In this section we shall exemplify properties of the near-singularity wave (6) numerically. We shall calculate *S* waves excited by a point source and propagating in a TI medium. We shall model the wavefield by the zeroth-order ray approximation (when the near-singularity wave is neglected) and by the far-field ray approximation (when the near-singularity wave is considered). Both ray approximations will be compared with the exact solution calculated by evaluating formula (1) numerically. We shall use two models displaying TI: a medium with cracks and Mesaverde immature sandstone. The medium with cracks is assumed to be formed by an isotropic host rock with the *P* and *S* velocities and the density α = 4.50 km/s, β = 2.53 km/s and ρ=2.8 g/cm^3. The host rock contains aligned thin water-filled cracks with the crack density e = 0.1 and the aspect ratio d = 0.001. The resultant density-normalized elastic parameters of the cracked medium calculated by the Hudson model (1981) are: a_{11}= 20.22, a_{33}= 20.04, a_{13}= 7.41, a_{44}= 5.10 and a_{66}=6.38 . Anisotropy of the *P* wave is 3.5 per cent, anisotropy of the *SV* and *SH* waves is 11.2 per cent (see Fig. 2). Shearer & Chapman (1989) use a similar cracked model (in their notation Model 1), but they use a different orientation of the symmetry axis and they assume also a non-zero velocity gradient. The second model, Mesaverde immature sandstone (Thomsen 1986), has the following elastic parameters: a_{11}= 22.36, a_{33}= 18.91, a_{13}= 8.49, a_{44}= 6.61, a_{66}=8.00 and ρ=2.46 g/cm^3. Anisotropies of the *P*, *SV* and *SH* waves for this model reach 8.3, 4.6 and 9.5 per cent, respectively (see Fig. 2).

For calculating the wavefield in the medium, we use the single point force $\mathbf{F}(t)=\mathbf{F}\cdot f(t)$, where $\mathbf{F}$ is the force vector, and $f(t)$ is the source-time function, which is defined as follows:

$$f(t)=\sin^2\left(\frac{\pi t}{T}\right) \text{ for } t\in\langle 0,T\rangle ,$$

for the other times $f(t)$ being zero. The source-time function has been chosen so that the wave has the form of a one-sided pulse in the far-field approximation. For parameter *T* specifying the pulse width, the value $T = 1\text{s}$ was used. The force vector was chosen as $\mathbf{F}=(1,\,1,\,0)^T$.

Figures 3 and 4 show waveforms and particle motions of the *S* waves propagating in the cracked medium and in the sandstone and recorded at four observation points that lie in the *x*-*z* plane at the distance from the source: r = 225.8 km for the cracked medium, and r = 257.1 km for the sandstone. This distance corresponds to 100 wavelengths of the *S* wave propagating in the direction of the symmetry axis of the medium. We used this enormously large distance to be sure that the far-field condition is well satisfied. Rays to the four observation points deviate from the symmetry axis by angles: $\vartheta = 2°$, 8°, 14° and 20°. We can see from figures 3 and 4 that the *S* waves separate differently at different observation points. As expected, almost no separation between the *SV* and *SH* waves is observed for the closest observation point to the singular direction with angle $\vartheta = 2°$. The separation time (difference in the arrival times of the *SV* and *SH* waves) for this point is only $dt = 0.02\ T$ for the cracked medium, and $dt = 0.05\ T$ for the sandstone, where T is the width of the *S* pulse. On the contrary, for the point with $\vartheta = 20°$ the *SV* and *SH* waves are fully separated in time: $dt = 1.61\ T$ for the cracked medium, and $dt = 3.62\ T$ for the sandstone.

Comparing the exact and ray solutions we found that the exact solution and the far-field ray solution coincide within the width of the line. This fact verifies that the *ray solution which considers the near-singularity wave describes correctly the S waves in the far field*. Comparing the far-field and the zeroth-order ray solutions we can see that the zeroth-order ray solution produces significant errors in amplitudes as well as in polarizations of the *S* waves, in particular, in the vicinity of the singular direction. Emphasize that the both media under study can be considered as weakly anisotropic. For materials displaying stronger anisotropy, these errors can be even larger. Close to the singular direction, when the *S* waves do not separate, the near-singularity wave affects mainly the predominant polarization of the *S* wave. The fact that the actual predominant polarization of *S* waves can remarkably differ from the polarization predicted by the zeroth-order ray approximation has been already reported (but not explained) by Vavryčuk (1992, Fig.13b). For directions, for which the *S* waves separate, the zeroth-order ray approximation predicts a linear polarization of the split *S* waves, but the near-singularity wave causes their ellipticity. For an increasing separation time between the split *S* waves, the ellipticity decreases.

4 CONCLUSION

We studied the exact solution and the approximate ray solutions of the wavefield generated by a point source in a homogeneous transversely isotropic medium and propagating in directions close to a kiss singularity. We found that the zeroth-order ray theory fails for these directions. A cause of this failure is an existence of a non-geometrical wave propagating from the source and having significant amplitudes in the directions close to a kiss singularity. This wave is described by the first-order ray approximation, being thus neglected by the zeroth-order ray theory. Surprisingly, *this wave can be of high frequency and it can be detected in the far field*. Physically, this wave is caused by an interaction of the split *S* waves and appears in times between arrivals of the split *S* waves. In analogy to the near-field wave, which appears in the vicinity of the point source, we call this wave as the *near-singularity wave*, because it is pronounced mainly for the directions close to the singularity. The near-singularity wave can affect amplitudes and polarization of the *S* waves in the near field as well as in the far field. If the *SV* and *SH* waves are not well separated, thus forming only one *S* wave, the near-singularity wave can change the predominant direction of the *S*-wave polarization. If the *SV* and *SH* wave are separated in time, then the near-singularity wave can cause that both split *S* waves are elliptically polarized. The ellipticity of the split *S* waves decreases with increasing separation time. The amplitude of the near-singularity wave depends on the strength of anisotropy: for isotropy the wave vanishes. On numerical examples we show that for weakly anisotropic TI media commonly used in modelling in crustal seismology the near-singularity wave can affect remarkably the *S* waves propagating in the directions up to 15° from the kiss singularity at distances up to hundreds of wavelengths from the source.

It is very like that the existence of the near-singularity wave is not confined only to homogeneous anisotropic media, but it will appear also in inhomogeneous anisotropic media. Therefore, any modelling of the wavefield in the homogeneous as well as inhomogeneous anisotropic media based on the ray theory or on its modifications like the quasi-isotropic approximation (Pšenčík 1998; Zillmer, Kashtan & Gajewski 1998), should in future take into account the near-singularity wave, in order to reproduce the wavefield near the kiss singularity properly.

Acknowledgements

The work was supported by the Grant Agency of the Czech Republic, Grant No. 205/96/0968, by the EC INCO-Copernicus Project IC15 CT96 200, and by the consortium project "Seismic waves in complex 3-D structures".

References

Burridge, R., 1967. The singularity on the plane lids of the wave surface of elastic media with cubic symmetry, *Q. J. Mech. appl. Math.*, **20**, 41-56.

Crampin, S., 1991. Effects of point singularities on shear-wave propagation in sedimentary basins, *Geophys. J. Int.*, **107**, 531-543.

Crampin, S. & M. Yedlin, 1981. Shear-wave singularities of wave propagation in anisotropic media, *J. Geophys.*, **49**, 43-46.

Červený, V., 1997. *Seismic Waves in Complex 3-D Structures - Report 5*. Department of Geophysics, Charles University, Prague.

Červený, V., Molotkov, I. & I. Pšenčík, 1977. *Ray Method in Seismogy*, Charles University Press, Prague.

Chapman, C. H. & P. M. Shearer, 1989. Ray tracing in azimuthally anisotropic media – II. Quasi-shear wave coupling, *Geophys. J.* , **96**, 65-83.

Coates, R. T. & C. H. Chapman, 1990. Quasi-shear wave coupling in weakly anisotropic 3-D media, *Geophys. J. Int.*, **103**, 301-320.

Hudson, J. A., 1981. Wave speeds and attenuation of elastic waves in material containing cracks, *Geophys. J. Roy. Astr. Soc.*, **64**, 133-150.

Kendall, J-M., Guest, W. S. & Thomson, C. J., 1992. Ray-theory Green's function reciprocity and ray-centred coordinates in anisotropic media, *Geophys. J. Int.,* **108**, 364-371.

Mura, T., 1991. *Micromechanics of Defects in Solids*. Kluwer Academic Publishers, London.

Payton R. G., 1977. Symmetry-axis elastic waves for transversely isotropic media, *Q. Appl. Math.*, **35,** 63-73.

Payton, R. G., 1983. *Elastic Wave Propagation in Transversely Isotropic Media*, Martinus Nijhoff Publishers, The Hague.

Pšenčík, I., 1998. Green functions for inhomogeneous weakly anisotropic media, *Geophys. J. Int.*, accepted for publication.

Rümpker, G. & C. J. Thomson, 1994. Seismic-waveform effects of conical points in gradually varying anisotropic media, *Geophys. J. Int.*, **118**, 759-780.

Shearer, P. M. & C. H. Chapman, 1989. Ray tracing in azimuthally anisotropic media – I. Results for models of aligned cracks in the upper crust, *Geophys. J.*, **96**, 51-64.

Thomsen, L., 1986. Weak elastic anisotropy, *Geophysics*, **51**, 1954-1966.

Vavryčuk, V., 1992. Polarization properties of near-field waves in homogeneous isotropic and anisotropic media: numerical modelling, *Geophys. J. Int.*, **110**, 180-190.

Vavryčuk, V., 1997. Elastodynamic and elastostatic Green tensors for homogeneous weak transversely isotropic media, *Geophys. J. Int.*, **130**, 786-800.

Vavryčuk, V. & Yomogida, K., 1995. Multipolar elastic fields in homogeneous isotropic media by higher-order ray approximations, *Geophys. J. Int.*, **121**, 925-932.

Vavryčuk, V. & Yomogida, K., 1996. *SH*-wave Green tensor for homogeneous transversely isotropic media by higher-order approximations in asymptotic ray theory, *Wave Motion*, **23**, 83-93.

Wang, C.-Y. & Achenbach, J. D., 1994. Elastodynamic fundamental solutions for anisotropic solids, *Geophys. J. Int.*, **118**, 384-392.

Zillmer, M., Kashtan, B. M. & D. Gajewski, 1998. Quasi-isotropic approximation of anisotropic ray theory, *Geophys. J. Int.*, **132**, 643-653.

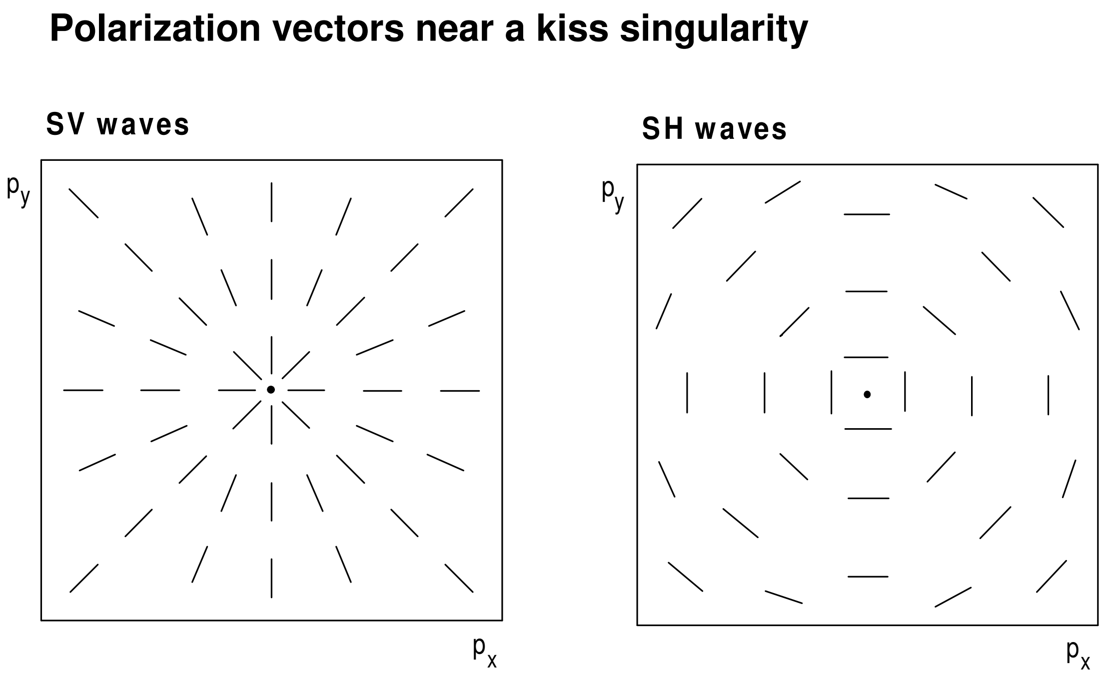

Figure 1. Horizontal projections of polarization vectors of the *SV* and *SH* waves near a kiss singularity in the p_x-p_y plane, where p_x and p_y are the horizontal components of the slowness vector.

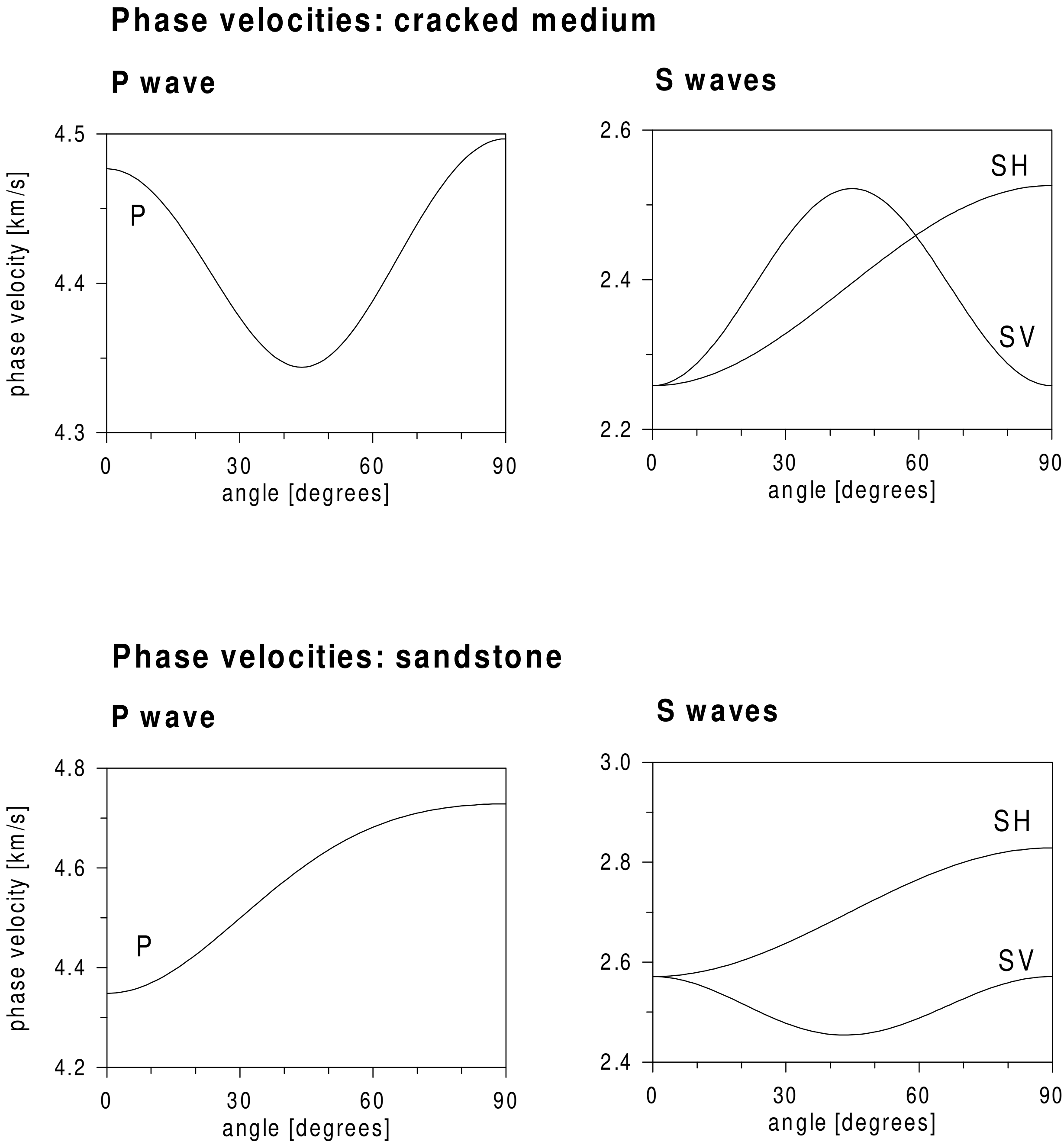

Figure 2. Phase velocities of the *P*, *SV* and *SH* waves as a function of the angle between the phase normal and the symmetry axis for the cracked medium and Mesaverde immature sandstone.

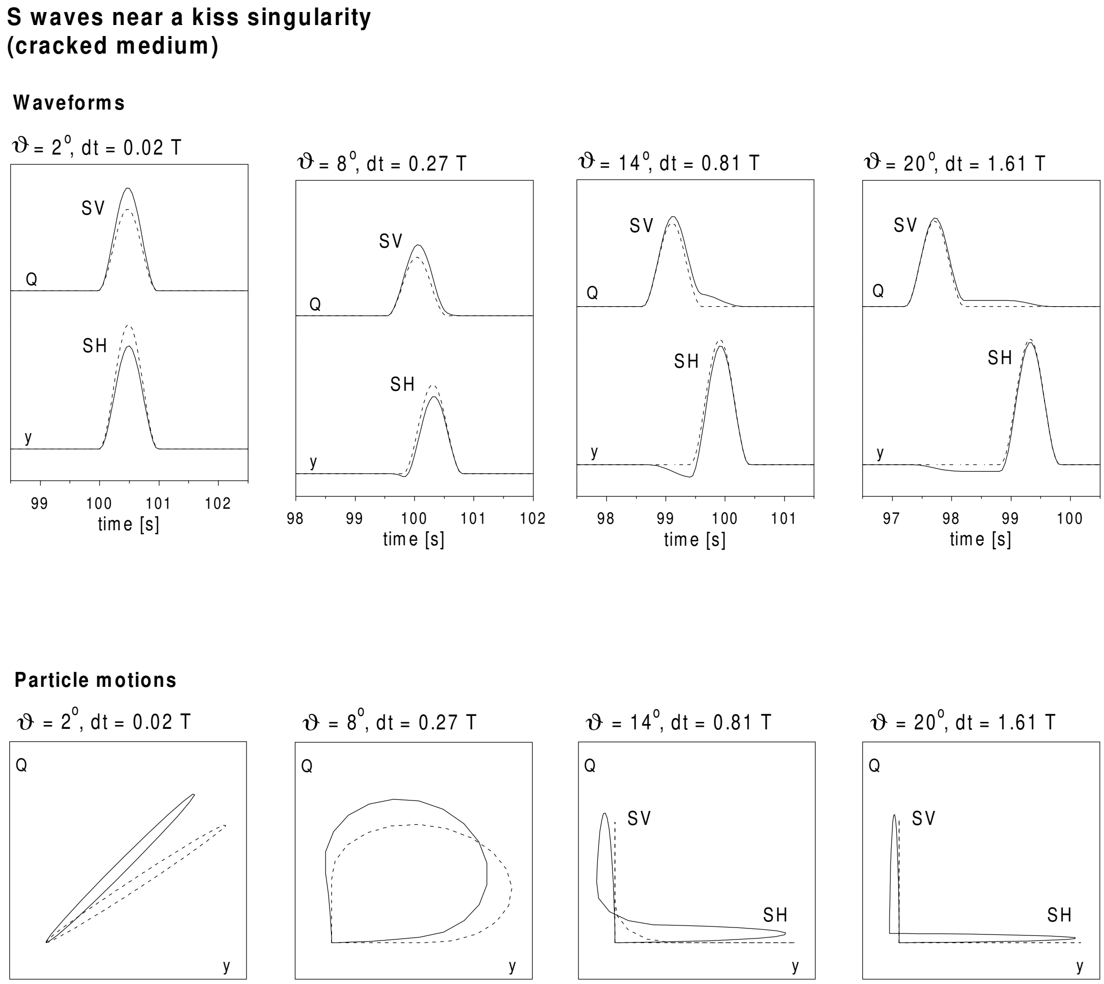

Figure 3. Waveforms and particle motions of S waves propagating in the cracked medium. Diagrams are shown for four receivers lying in the x-z plane at distance r = 225.8 km from the source and at rays deviating from the kiss singularity by ϑ = 2°, 8°, 14° and 20°. Parameter dt is the delay time between SV- and SH-wave arrivals, T is the width of the signal, T = 1s.. Component Q lies in the x-z plane and is perpendicular to the ray. Dashed line – zeroth-order ray solution, full line – exact solution and/or far-field ray solution.

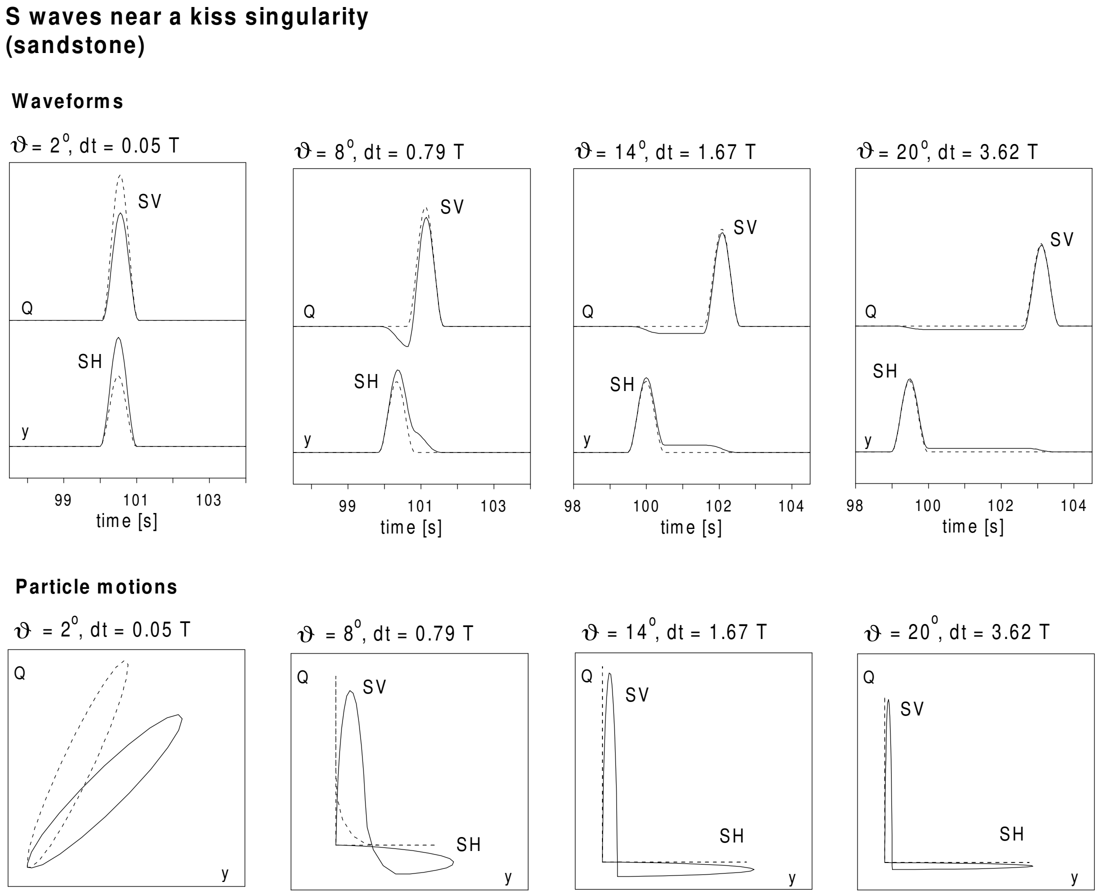

Figure 4. Waveforms and particle motions of S waves propagating in Mesaverde immature sandstone. Receivers lie at distance r = 257.1 km from the source. Dashed line – zeroth-order ray solution, full line – exact solution and/or far-field ray solution.